

L. P a r a s h k e v o v a

Dynamic Penetration and Perforation of Plates by a Rigid Cylindrical Cone Tip Projectile

Many technological operations like cutting, piercing, perforating as well as some problems connected with the reliability of vehicles or defence devices in emergency lead to the need of studying the penetration process of a rigid indenter into target material. The initial velocities and the tip of the projectiles may vary in a wide range.

The penetration process of a rigid cylindrical cone tip projectile into a perfectly-plastic plate at initial impact velocities between 100 - 900 m/s will be discussed.

The approach used here is similar to that described in [1] for blunt cylindrical projectiles only. It assumes creating of different Kinematically Admissible Velocity Fields (KAVF) of plastic flow, modelling the plate material motion during the penetration.

The power of the true forces \dot{W} needed for the deformation of the plate material is estimated by (1):

$$(1) \quad \dot{W} \leq \dot{W}^* = \tau_s \sum_j \int_{\Omega_j} \sqrt{2\dot{e}_{lk}^{(j)}\dot{e}_{lk}^{(j)}} d\Omega + \tau_s \sum_j \int_{S_j} [v_{\tau}^{(j)}] ds + \frac{dK}{dt},$$

where $\frac{dK}{dt}$ is the kinetic energy rate of the moving material, given by:

$$(2) \quad \frac{dK}{dt} = \frac{\rho}{2} \sum_j \left\{ \int_{\Omega_j} \frac{\partial [v_1^{(j)} v_1^{(j)}]}{\partial t} d\Omega + \int_{S_j} v_n^{(j)2} dS + \int_{S_j} [v_{\tau}^{(j)2}] |v_n^{(j)} - v_{ns}^{(j)}| dS \right\}$$

The right hand side of this inequality (1) provides an upper bound of the real forces and may be obtained from every kind of kinematically admissible velocity fields available - with or without any discontinuities [2]. In (1) and (2) the

subscript (j) refers to the subdomains, which the whole target material is divided into, for the different KAVF proposed. For subscripts k and l Einstein's rule for summing is used. All velocity components are kinematically admissible.

$v_n^{(j)}$ - normal velocity component of material particles on the surface S_{γ_j}

$\left[v_\tau^{(j)} \right]$ - discontinuity of tangential velocity components of material particles on both sides of the surface S_{γ_j}

$v_{ns}^{(j)}$ - normal component of the velocity, the surface S_{γ_j} itself moves with.

$\dot{e}_{1m}^{(j)}$ - strain rate components, received from KAVF in the subdomain Ω_j

All KAVF must be created subject to the following restrictions:

1. On the contact surface between the projectile and the plate material their velocities coincide at each moment;
2. Incompressibility condition:

$$\frac{\partial v_r}{\partial r} + \frac{v_r}{r} + \frac{\partial v_z}{\partial z} = 0,$$

3. Equality of normal velocities on both sides of S_{γ_j} , where S_{γ_j} is the surface of velocity discontinuities, which could be an internal boundary between the subzones moving in a different way, as well as a boundary separating a moving zone from the other part of the dead material.

Let the parameters of the projectile be:

a - radius of the cylindrical part;

$\bar{\gamma}$ - vertex angle of the conical tip; $\gamma = \frac{\pi}{2} - \bar{\gamma}$; $\gamma \in (0, \frac{\pi}{2})$

v_p - velocity at the moment t ; m - mass;

and let those of the plate be:

H - thickness; τ_s - yield limit; ρ - density.

Let us assume that at the moment t the indenter has reached the depth h , then for $t > 0$, $\dot{h}(t) = v_p(t)$ holds. All the time the projectile moves straight perpendicularly to the plate. Because of the axial symmetry of the problem the cylindrical coordinate system, connected with the back side of the plate is introduced. Two independent admissible schemes for modelling the behaviour of the plate material at the indenter invasion are assumed. In essence scheme A (Fig.1) presents the case of projectile penetration into half-space. The material is being pushed along the indenter through the upper free plate surface. There is no influence of the back free plate surface. In scheme B the

material is coming down in a manner, shown in Fig.3 and the back side mentioned

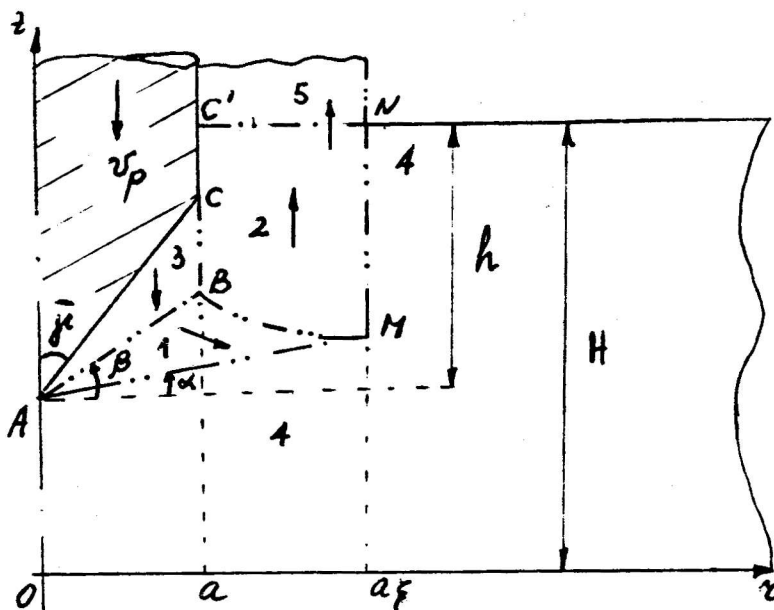


Fig. 1

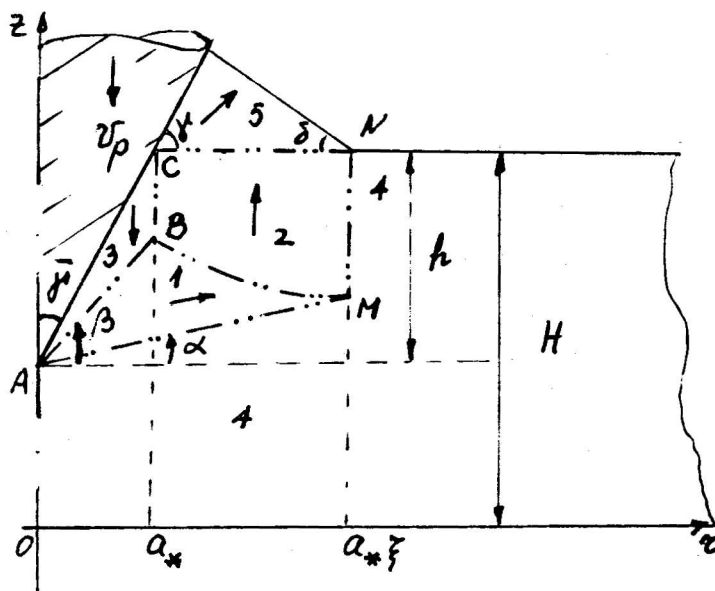


Fig.2

affects this motion. Formulae for the velocity fields in the corresponding subdomains are given by (3) for scheme A and by (4) for scheme B.

$$(3) \quad \begin{cases} v_r^{(1)} = -\frac{v_p}{2B} & v_z^{(1)} = -\frac{v_p}{2B} \left[2\operatorname{tg}\alpha - \frac{z-H+h}{r} \right]; & v_r^{(2)} = 0 & v_z^{(2)} = -\frac{v_p}{A}; \\ v_r^{(3)} = 0 & v_z^{(3)} = -v_p; & v_r^{(4)} = 0 & v_z^{(4)} = 0. \end{cases}$$

$$(4) \quad \begin{cases} v_r^{(1)} = -\frac{v_p}{2Y} N_4 r & v_z^{(1)} = v_p \left[N_4 \frac{H-h-z}{a} + \frac{3Ar}{2\xi^3 a} - 1 \right]; & v_r^{(3)} = 0 & v_z^{(3)} = -v_p \\ v_r^{(2)} = 0 & v_z^{(2)} = v_p \left[\frac{3Ar}{2\xi^3 a} - 1 \right]; & v_r^{(4)} = 0 & v_z^{(4)} = 0. \end{cases}$$

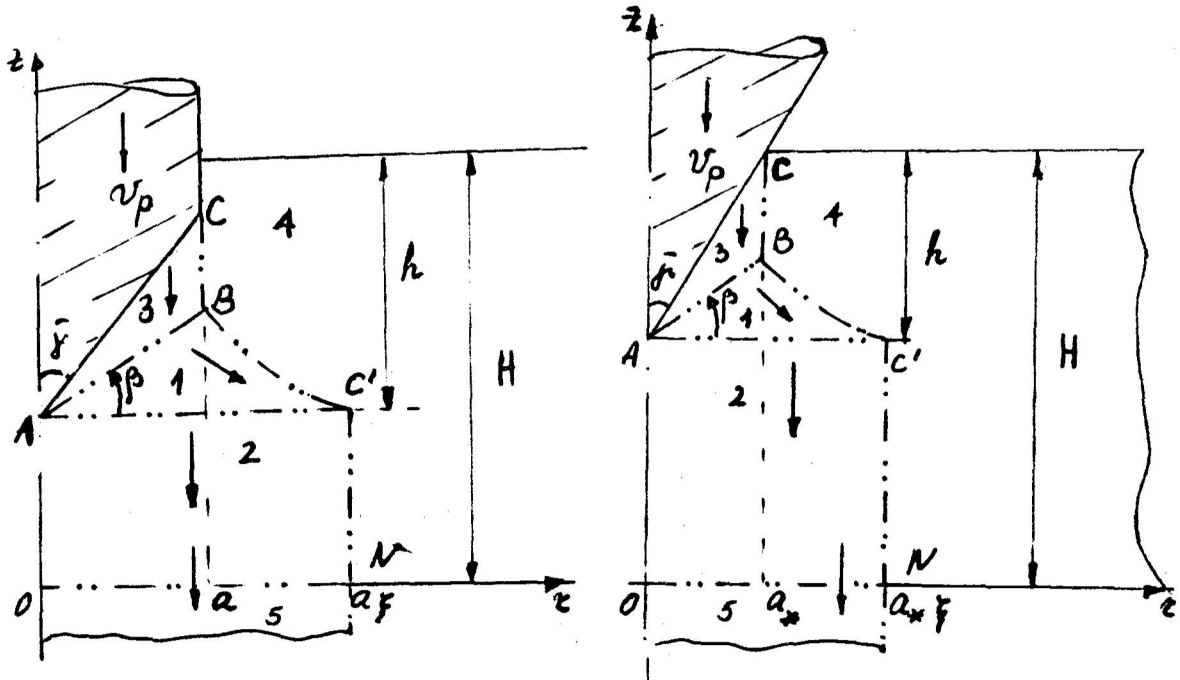


Fig.3

The specific geometry of the projectile requires the consideration of two stages of the process for both variants of deformation to be taken into account. The first stage continues up to the moment when only the conical part of the

projectile has penetrated into the plate. In this case for scheme **B** formulae (4) hold if a is replaced by $a_* = h \cdot \cotg \gamma$. However, for scheme **A** an other KAVF must be designed so that the part of the material coming out not to conflict with the moving conical part of the projectile. The KAVF illustrated in Fig.2 and given by formulae (3) completed by (5) satisfy that requirement.

$$(5) \quad \begin{cases} v_r^{(5)} = v_p \frac{a_*}{r} \cotg \gamma & v_z^{(5)} = \frac{v_p}{A}, \quad \text{tg} \delta = N_3 \text{tg} \gamma \end{cases}$$

The surfaces between zones 1,2 are formed by the curve L_{BM} (Fig.1) and between zones 1,4 - by the curve $L_{BC'}$ (Fig.3). Expressions (6) for L_{BM} and (7) for $L_{BC'}$ are the solutions of two simple differential equations reflecting restriction 3 for scheme **A** and scheme **B** respectively.

$$(6) \quad z_{BM} = \frac{a^2}{2r} \xi^2 N_2 + N_1 r + H - h,$$

$$(7) \quad z_{BC'} = \frac{a^3}{N_4} \left[\frac{1}{r^2} - \frac{1}{a^2} \right] + r \text{tg} \beta + H - h.$$

The fields (3), respectively (3) and (5), applied to (1) estimate from above the true forces on the projectile. So in case **A** we have $\dot{W}^* = \pi a^2 v_p P_A$ and :

$$(8) \quad \pi a^2 v_p P_A = M_{AD} + M_{AS} + K_A, \quad \text{where:}$$

M_{AD} - power of plastic deformations;

M_{AS} - power on the surfaces of velocity discontinuities

$K_A = dK/dt$ - kinetic energy rate in the plastic domain.

$$(9) \quad M_{AD} = \pi a^2 v_p \tau_s \frac{1}{4} (J_1 + J_2 + J_3) \quad \text{and}$$

$$J_1 = \frac{1}{B} \left[\frac{\text{tg} \beta}{4} \sqrt{\text{tg}^2 \beta + 4} - \frac{\text{tg} \alpha}{4} \sqrt{\text{tg}^2 \alpha + 4} + \ln \frac{l_1}{l_2} \right]$$

$$J_2 = \frac{\xi^2}{A} \left\{ \left[\frac{\text{tg} \alpha}{4} \sqrt{\text{tg}^2 \alpha + 4} + \ln l_2 \right] \frac{A}{B \xi^2} - \left[\frac{\text{tg} \beta}{4} \sqrt{\text{tg}^2 \beta + 4} + \ln l_1 \right] \frac{A}{B \xi^2} + \right.$$

$$\left. + \frac{1}{2} \left[N_1^2 \ln \frac{l_2}{l_1} + \frac{N_1(N_1+1)}{2} \ln \frac{l_1^2 - N_1 l_1 - 1}{l_2^2 - N_1 l_2 - 1} + \frac{1}{l_1} - \frac{1}{l_2} + l_1 - l_2 \right] \right\}$$

$$J_3 = \frac{\xi^2 N_1^2}{A \sqrt{N_1^2 + 4}} \ln \frac{(2l_2 - N_1 + \sqrt{N_1^2 + 4})(2l_1 - N_1 - \sqrt{N_1^2 + 4})}{(2l_2 - N_1 - \sqrt{N_1^2 + 4})(2l_1 - N_1 + \sqrt{N_1^2 + 4})}$$

$$(10) \quad M_{AS} = \pi a^2 \dot{v}_p \sum_{i=4}^8 J_i \quad \text{and}$$

$$J_4 = \frac{\xi^2}{2B}(\text{tg}^2 \beta + 1), \quad J_5 = \frac{2\xi}{A} \left(\frac{h}{a} - \xi \text{tg} \alpha \right),$$

$$J_6 = \frac{2\xi^2}{A} \left[B - \frac{1}{2} N_1 \ln \xi + \frac{A^2(N_1^2 + 1)}{B\xi^2} \right], \quad J_7 = \frac{1}{2B \cos^2 \beta}, \quad J_8 = \frac{2\xi^2}{A} Y;$$

$$(11) \quad K_A = \pi a^2 \dot{v}_p \rho \sum_{i=1}^7 G_i \quad \text{and}$$

$$G_1 = \frac{2}{3} a \dot{v}_p Y, \quad G_2 = 0, \quad G_3 = \frac{\xi^3 \dot{v}_p^2}{8B^2 \cos^2 \alpha};$$

$$G_4 = \frac{\dot{v}_p^2 \xi^4}{8A^2 B} \left| -B + 4(N_1 + N_2) \ln \xi - \frac{A^2(N_1^2 + 2N_1 N_2 + 1)}{B\xi^2} \right|,$$

$$G_5 = \frac{2a \dot{v}_p}{A(\xi + 1)} \left[\frac{h}{2a}(\xi + 1) - \frac{\xi^2 N_2}{2} - \frac{N_1}{3}(\xi^2 + \xi + 1) \right], \quad G_6 = \frac{a \dot{v}_p}{A^2} \left[\frac{h}{a} - \frac{2}{3} \text{tg} \gamma \right],$$

$$G_7 = \frac{1}{2B^2} \sum_{i=1}^6 Q_i \quad \text{and}$$

$$Q_1 = a \dot{v}_p \left(1 + 4 \text{tg}^2 \alpha \right) \frac{B}{3} \left[1 + \frac{1}{A} (\xi - 1)^2 (2\xi + 1) \right],$$

$$Q_2 = -4a \dot{v}_p \text{tg} \alpha (Q_{21} + Q_{22}), \quad \text{where:}$$

$$Q_{21} = \frac{1}{6} (\text{tg}^2 \beta - \text{tg}^2 \alpha),$$

$$Q_{22} = \left| \frac{\xi^3}{8} (\xi - 1) N_2^2 + \frac{\xi^2}{2} (\xi - 1) N_1 N_2 + \frac{1}{6} (\xi^3 - 1) (N_1^2 - \text{tg}^2 \alpha) \right|,$$

$$Q_3 = a \dot{v}_p (Q_{31} + Q_{32}), \quad \text{where:}$$

$$Q_{31} = \frac{1}{9}(\text{tg}^3 \beta - \text{tg}^3 \alpha) ,$$

$$Q_{32} = \left| \frac{\xi^3}{8}(\xi^3 - 1)N_2^3 + \frac{\xi^3}{4}(\xi - 1)N_2^2 + \frac{\xi^2}{2}(\xi - 1)N_1^2 N_2 + \frac{1}{9}(\xi^3 - 1)(N_1^3 - \text{tg}^3 \alpha) \right| ,$$

$$Q_4 = \frac{-v^2}{B} \xi^2 N_2 \ln \xi \cdot \text{tg} \alpha \cdot \text{tg} \beta ,$$

$$Q_5 = \frac{v^2}{B} (\text{tg} \beta - \text{tg} \alpha) (Q_{51} - Q_{52}) \quad \text{where:}$$

$$Q_{51} = \frac{1}{4}(\text{tg}^2 \beta - \text{tg}^2 \alpha) , \quad Q_{52} = \left| \frac{1}{4} A \xi^2 N_2^2 + \frac{\xi^2}{2} N_1 N_2 \ln \xi + \frac{1}{4} A (N_1^2 - \text{tg}^2 \alpha) \right|$$

$$Q_6 = \frac{-v^2}{2B} (Q_{61} + Q_{62}) \quad \text{where:}$$

$$Q_{61} = \frac{1}{6}(\text{tg}^3 \beta - \text{tg}^3 \alpha) ,$$

$$Q_{62} = \left| \frac{\xi^2}{6}(\xi^4 - 1)N_2^3 + \frac{\xi^2}{2} A N_1 N_2^2 + \frac{\xi^2}{2} N_1^2 N_2 \ln \xi + \frac{1}{6} A (N_1^3 - \text{tg}^3 \alpha) \right| ,$$

As it was already noted, the process in scheme A is rather different until $h < a \cdot \text{tg} \gamma$. For this earlier stage the estimate of the forces on the projectile $\pi a_*^2 v_p \tilde{P}_A$ is obtained from (1),(3) and (5), as follows:

$$(12) \quad \pi a_*^2 v_p \tilde{P}_A = \tilde{M}_{AD} + \tilde{M}_{AS} + \tilde{K}_A , \quad a_* = h \cdot \text{cotg} \gamma, \quad \text{where:}$$

$$(13) \quad \tilde{M}_{AD} = M_{AD} \Big|_{a=a_*} + \pi a_*^2 v_p \tau_s J_9 ,$$

$$J_9 = 4 \left[\xi N_3 \ln \xi - (\xi N_3 + 1) \ln \frac{\xi N_3 + 1}{N_3 + 1} \right]$$

$$(14) \quad \tilde{M}_{AS} = M_{AS} \Big|_{a=a_*} + \pi a_*^2 v_p \tau_s 2(\xi - 1) \text{cotg} \gamma ,$$

$$(15) \quad \tilde{K}_A = \pi a_*^2 v_p \rho \sum_i G_i , \quad i = 1, 3, 4, 5, 7, 8, 9, 10$$

$$G_8 = \frac{\dot{v}_p a_* \operatorname{tg} \gamma}{3A^2} \left[1 + \xi^3 N_3 - \frac{(1 + \xi N_3)^3}{(1 + N_3)^2} \right] + 2v_p^2 \operatorname{cotg}^2 \gamma \left[1 + \frac{N_3}{\xi} - \frac{(1 + N_3)^2}{(1 + \xi N_3)} \right] + \frac{1}{2} (\dot{v}_p a_* + v_p^2 \operatorname{cotg} \theta) J_9 \operatorname{cotg} \gamma ,$$

$$G_{10} = v_p^2 \frac{1}{pA} \operatorname{cotg}^2 \gamma \ln \xi .$$

In the same way from the fields (4) the estimate $\pi a^2 v_p P_B$ for case B (16) is obtained, where:

$$(16) \quad \pi a^2 v_p P_B = M_{BD} + M_{BS} + K_B$$

M_{BD} - power of plastic deformations;

M_{BS} - power on the surfaces of velocity discontinuities

$K_B = dK/dt$ - kinetic energy rate in the plastic domain.

$$(17) \quad M_{BD} = \pi a^2 v_p \tau_s (B_1 + B_2) ,$$

$$B_1 = \sqrt{\frac{4}{3} + \operatorname{tg}^2 \beta} (3 \ln \xi - \frac{A}{2}) , \quad B_2 = \frac{3A}{2\xi^3} \left[\xi^2 \frac{2H}{a} - \frac{h}{a} A - \frac{2}{3} \operatorname{tg} \gamma \right] .$$

$$(18) \quad M_{BS} = \pi a^2 v_p \tau_s \sum_{i=3}^7 B_i , \text{ where:}$$

$$B_3 = \frac{1}{3} (\xi^3 - 1) N_4 (\operatorname{tg}^2 \beta + 1) - 4 \operatorname{tg} \beta \ln \xi , \quad B_4 = \frac{1}{3} N_4 ,$$

$$B_5 = \frac{A-2}{a\xi} (H-h) , \quad B_6 = \frac{N_4}{3 \cos^2 \beta} , \quad B_7 = 2Y .$$

$$(19) \quad K_B = \pi a^2 v_p \rho \sum_{i=1}^6 I_i , \text{ where:}$$

$$I_1 = \frac{1}{40} N_4^2 \xi^3 \operatorname{tg} \beta (5 - \xi^2) [\dot{v}_p a + v_p^2 (\frac{1}{2} N_4 - \operatorname{cotg} \theta)] ,$$

$$I_2 = 2N_4^2 \left\{ \dot{v}_p a \left(\frac{9}{4} \operatorname{tg}^2 \beta F_1 - \frac{3 \operatorname{tg} \beta}{N_4} F_2 + \frac{1}{N_4^2} F_3 + F_4 - 3 \operatorname{tg} \beta F_5 + \frac{2}{N_4} F_6 \right) + \right.$$

$$\begin{aligned}
 & + v_p^2 \left[\frac{9}{4} \theta^2 \operatorname{tg}^2 \beta F_1 + \frac{3}{2N_4} \theta^2 \operatorname{tg} \beta F_2 + \frac{3}{2} (\theta_1 + \theta_2) \operatorname{tg} \beta F_5 - \theta_1 \left(F_4 + \frac{F_6}{N_4} \right) \right] \Big\} \\
 F_1 &= \frac{A}{2N_4} - \frac{\xi^4 - 1}{4N_4} + \frac{\xi^5}{5} \operatorname{tg} \beta, \quad F_2 = \frac{\xi - 1}{N_4} - \frac{\xi^3 - 1}{3N_4} + \frac{\xi^4}{4} \operatorname{tg} \beta, \\
 F_3 &= \frac{1 \ln \xi}{N_4} - \frac{A}{2N_4} + \frac{\xi^4}{4} \operatorname{tg} \beta, \\
 F_4 &= \frac{1}{N_4^3} \left[\frac{\xi^4 - 1}{12\xi^4} - \frac{A}{2\xi^2} + \ln \xi - \frac{A}{6} \right] + \frac{\operatorname{tg} \beta}{N_4^2} \left[\frac{\xi - 1}{\xi} - 2(\xi - 1) + \frac{\xi^3 - 1}{3} \right] + \\
 & + \frac{\operatorname{tg}^2 \beta}{N_4} \left[\frac{A}{2} - \frac{\xi^4 - 1}{4} \right] + \frac{\xi^5}{15} \operatorname{tg}^3 \beta, \\
 F_5 &= \frac{1}{2N_4^2} \left[\frac{\xi - 1}{\xi} - 2(\xi - 1) + \frac{\xi^3 - 1}{3} \right] + \frac{\operatorname{tg} \beta}{N_4} \left[\frac{A}{2} - \frac{\xi^4 - 1}{4} \right] + \frac{\xi^5}{10} \operatorname{tg}^2 \beta, \\
 F_6 &= \frac{1}{2N_4^2} \left[\frac{A}{2\xi^2} - 2 \ln \xi + \frac{\xi^2 - 1}{2} \right] + \frac{\operatorname{tg} \beta}{N_4} \left[\xi - 1 - \frac{\xi^3 - 1}{3} \right] + \frac{\xi^4}{8} \operatorname{tg}^2 \beta. \\
 I_3 &= v_p^2 A \left[\frac{A}{16} (\operatorname{tg}^2 \beta + 1) N_4^2 + \frac{\xi + 1}{\xi^3} + \frac{3A^2 \operatorname{cotg}^2 \beta}{40\xi^4} \right], \\
 I_4 &= \frac{H-h}{8\xi^2} \dot{v}_p (\xi^4 - 2\xi^2 + 9) + \frac{v_p^2}{a} (9 - \xi^2) A \operatorname{cotg} \theta, \quad I_5 = \frac{2}{3} a \dot{v}_p Y, \\
 I_6 &= \left(\frac{h}{a} - \frac{2}{3} \operatorname{tg} \gamma \right) \frac{1}{8\xi^4} \dot{v}_p a (\xi^4 - 2\xi^2 + 9) + \frac{v_p^2 A (9 - \xi^2) \operatorname{cotg} \theta}{p}.
 \end{aligned}$$

In formulae (3) - (19) the following notations are used:

$$A = \xi^2 - 1, \quad Y = \operatorname{tg} \gamma - \operatorname{tg} \beta, \quad B = \operatorname{tg} \beta - \operatorname{tg} \alpha,$$

$$N_1 = \frac{\xi^2 \operatorname{tg} \alpha - \operatorname{tg} \beta}{A}, \quad N_2 = \frac{2B}{A}, \quad N_3 = \frac{3 - \xi^2 + (\xi - 1) \sqrt{(\xi - 1)(\xi + 3)}}{2\xi(2\xi - 3)}, \quad N_4 = \frac{A \operatorname{cotg} \beta}{\xi^3},$$

$$l_1 = \frac{1}{2} (\sqrt{\operatorname{tg}^2 \beta + 4} + \operatorname{tg} \beta), \quad l_2 = \frac{1}{2} (\sqrt{\operatorname{tg}^2 \alpha + 4} + \operatorname{tg} \alpha),$$

$$\theta_1 = \operatorname{cotg} \theta + N_4, \quad \theta_2 = \operatorname{cotg} \theta + \frac{1}{2} N_4$$

For the beginning stage ($h < a \operatorname{tg} \gamma$) of case **B** formulae (16) - (19) hold, if in them a is replaced by $a_* = h \cdot \cot \gamma$ and $\cot \theta = \cot \gamma$, P_B becomes \tilde{P}_B . When $h \geq a \operatorname{tg} \gamma$, $\cot \theta = 0$.

For both cases the integrals $\int_{\Omega_j} \frac{\partial}{\partial t} (v_i^{(j)} v_i^{(j)}) d\Omega$ in (2) are calculated

according to the assumption that for time period $\Delta t = t_i - t_{i-1}$ the variations of the parameters α , β and ξ (i.e. $\dot{\alpha}$, $\dot{\beta}$, $\dot{\xi}$) are negligible. So only the terms containing \dot{v}_p and \dot{h} give a considerable contribution.

The KAVF for scheme **A** have three free parameters: the angles α , β and dimensionless parameter ξ and those for scheme **B** have two free parameters: an angle β and ξ .

According to the basic inequality (1) it is clear that the aim of the method is to suggest such upper bound estimates as small as possible, i.e. closer to the true power needed for the deformation process. Thus a good way to improve each of the estimates (for case **A** or case **B**) is minimizing it with respect to the free parameters at every moment of the penetration concerned. Let α_* , β_* and ξ_* denote the values of the free parameters, which minimize the estimates P_A (or \tilde{P}_A), P_B (or \tilde{P}_B). These values are obtained subject to the following restriction intervals:

$$\text{scheme A } \begin{cases} \text{for } \alpha : 0 < \operatorname{tg} \alpha < \frac{2}{3} E \operatorname{tg} \gamma, & \begin{cases} E = 1 \text{ if } h < a \operatorname{tg} \gamma \\ E = 1.5 \text{ if } h \geq a \operatorname{tg} \gamma \end{cases} \\ \text{for } \beta : \operatorname{tg} \alpha < \operatorname{tg} \beta < \operatorname{tg} \gamma, & \begin{cases} \xi_1 = 1 \text{ if } h \geq a \operatorname{tg} \gamma \\ \xi_1 = 1.5 \text{ if } h < a \operatorname{tg} \gamma \end{cases} \\ \text{for } \xi : \xi_1 < \xi < \operatorname{tg} \gamma \cdot \cot \gamma, & \end{cases}$$

$$\text{scheme B } \begin{cases} \text{for } \beta : 0 < \operatorname{tg} \beta < \operatorname{tg} \gamma \\ \text{for } \xi : 1 < \xi < \sqrt{3} \end{cases}$$

Since no wave and thermal effects are considered, (which naturally constrains the field of applicability of the method used here) we assume that the projectile velocity reduces during the time according to Newton's equation of motion (20). We solve it numerically using small time steps.

$$(20) \quad m \dot{v}_p = -\pi a^2 P_{RM}(\alpha^*, \beta^*, \xi^*), \text{ where}$$

$$P_{RM} = \begin{cases} \min(\tilde{P}_A, \tilde{P}_B) \frac{a_*^2}{a^2} & \text{when } h < a \operatorname{tg} \gamma \\ \min(P_A, P_B) & \text{when } h \geq a \operatorname{tg} \gamma \end{cases}$$

The expression to the right hand side of (20) is the predicted resistant force on the projectile at the moment t , i.e. at the depth h . This force coincides with the smaller one of the estimates P_A and P_B . In other words

until $P_A < P_B$ the deforming plate material "prefers" to move following pattern A, and when $P_A \geq P_B$ it "prefers" scheme B. The choice of an appropriate scheme is based on its effectiveness with respect to minimizing the energy consumption. This way such a criterion, connected with the physical phenomenon of penetration, is doubtless much better than the geometric one, suggested in [3].

In the computer code implementing the above approach, the transition from scheme A to scheme B takes place automatically. For some correlation among the initial parameters it is possible to obtain that the material moves only according to scheme A (for example at comparatively low velocity and very thick plate) or at the other correlation among the same parameters - only the scheme B holds (for example at high velocity, sharp tip, thin plate).

As a result of the programme at least two goals become attainable: a) to predict the main parameters of the process in the course of time. Such parameters at each moment are: the depth and the current velocity of the penetrator, the plastic zones shape and sizes in the target material, the response forces, the duration of interacting (penetration or perforation). b) to estimate the influence of every initial parameter of the projectile (radius, initial velocity, angle of the cone part) on the process, the influence of a plate parameter (thickness, density, yield limit) on the ballistic velocity limit or the depth of the penetration as well.

R e f e r e n c e s:

1. П а р а ш к е в о в а, Л. Исследование проникания жесткого пуансона в плиту конечной толщины методом верхних оценок. — Материалы VI национального конгресса по механике, Варна, 1989, 190-194.
2. Theory of plastic deformation of metals. — Moscow, Mashinostroenie, 1983, 598. (in Russian)
3. R a v i d, M., R. B o d n e r. Dynamic perforation of viscoplastic plates by rigid projectiles. — Int. J. Engng. Sci., 21, 1983, 577-591.

Received on January 21, 1992